

# Microsilica or MgO grain size: Which one mostly affects the *in situ* spinel refractory castable expansion?

M.A.L. Braulio<sup>a</sup>, P.O.C. Brant<sup>b</sup>, L.R.M. Bittencourt<sup>b</sup>, V.C. Pandolfelli<sup>a,\*</sup>

<sup>a</sup> FIRE Associate Laboratory, Federal University of São Carlos, Materials Engineering Department, Materials Microstructural Engineering Group, km 235, Rod. Washington Luís, 13565-905 São Carlos, SP, Brazil

<sup>b</sup> Magnesita Refratários S.A., Research and Development Center, 240 Pr. Louis Ensck, Contagem, MG, Brazil

Received 13 March 2009; received in revised form 12 April 2009; accepted 25 May 2009

Available online 18 June 2009

## Abstract

Microsilica is commonly added to alumina–magnesia castables to counterbalance the *in situ* spinel expansion. This effect is attained by the generation of a low-melting temperature phase, which also affects the expansive reaction kinetics. Additionally, the  $\text{MgAl}_2\text{O}_4$  formation depends on the grain size of the reactants. The use of coarse magnesia grains results in lower  $\text{Mg}^{2+}$  dissolution and could lead, at 1500 °C, to forsterite development ( $\text{Mg}_2\text{SiO}_4$ ). For finer MgO, silica was detected at the edge of the spinel grains. Considering these aspects, this work evaluated the effect of microsilica content for different magnesia grain sizes (<45 or <100 μm). Due to a faster spinel formation for the fine MgO source, microsilica counterbalanced the  $\text{MgAl}_2\text{O}_4$  expansion. Conversely, for the coarser MgO, silica increased the  $\text{Mg}^{2+}$  dissolution, speeding up the spinel formation and expansion. Therefore, microsilica presented opposite roles, pointing out that it does not always counterbalance the spinel expansion. This work also indicated the need for a systemic approach for the expanding design of alumina–magnesia refractory castables.

© 2009 Elsevier Ltd and Techna Group S.r.l. All rights reserved.

**Keywords:** C. Thermal expansion; D. Spinel; D.  $\text{SiO}_2$ ; E. Refractories

## 1. Introduction

Microsilica is known by its counterbalancing effect on the *in situ* spinel ( $\text{MgAl}_2\text{O}_4$ ) disruptive expansion due to the softening mechanism associated with the liquid phase generation [1]. According to Nandi et al. [2] the liquid absence could lead to high expansion and porosity with the spinel formation.

A further role of silica in this sort of castables is its ability to speed up the high temperature reactions. The liquid phase formation increases the ion diffusion and, thus, promotes a faster spinel formation [3]. Despite these advantages, high liquid contents results in shrinkage, which could increase the crack generation [2,4]. As a consequence of this liquid at high temperatures, the refractoriness decreases, leading to lower castables' hot properties, such as the hot modulus of rupture [5,6] and the creep resistance [7]. Considering this aspect and also the associated shrinkage, Tawara et al. [8] proposed a balance between the magnesia and the silica content. According

to these authors, a high fine fraction  $\text{MgO}/\text{SiO}_2$  wt.% ratio (>12) results in huge permanent linear changes, whereas a lower one (<3) leads to shrinkage.

Nevertheless, another aspect disregarded in these analyses and that also influences the spinel formation kinetics is the grain size of the reactants. In previous publications of the authors [9,10], the reduction of the magnesia grain size led to a lower overall expansion and lower initial spinel formation temperature. Moreover, for coarser magnesia grains (<100 μm), an interaction between silica and magnesia was detected after firing at 1500 °C leading to phases predicted by local equilibrium diagrams, such as forsterite ( $\text{Mg}_2\text{SiO}_4$ ) [10]. For this MgO grain size, due to the lower  $\text{Mg}^{2+}$  dissolution and the reduction of the liquid phase content in the temperature range between 1300 and 1500 °C (inducing the  $\text{CA}_6$  formation) [11], silica and magnesia were available to react with each other.

For a fine magnesia grain size (<45 μm), microsilica behaved as expected and counterbalanced the *in situ* spinel formation. Fig. 1 presents the expansive behavior of CAC-bonded alumina–magnesia castables containing different microsilica amounts [7]. Compared to the reference (0 wt.% microsilica), low silica contents (0.25 or 0.5 wt.%) led to higher

\* Corresponding author. Tel.: +55 16 3351 8252.

E-mail address: [vicpando@power.ufscar.br](mailto:vicpando@power.ufscar.br) (V.C. Pandolfelli).

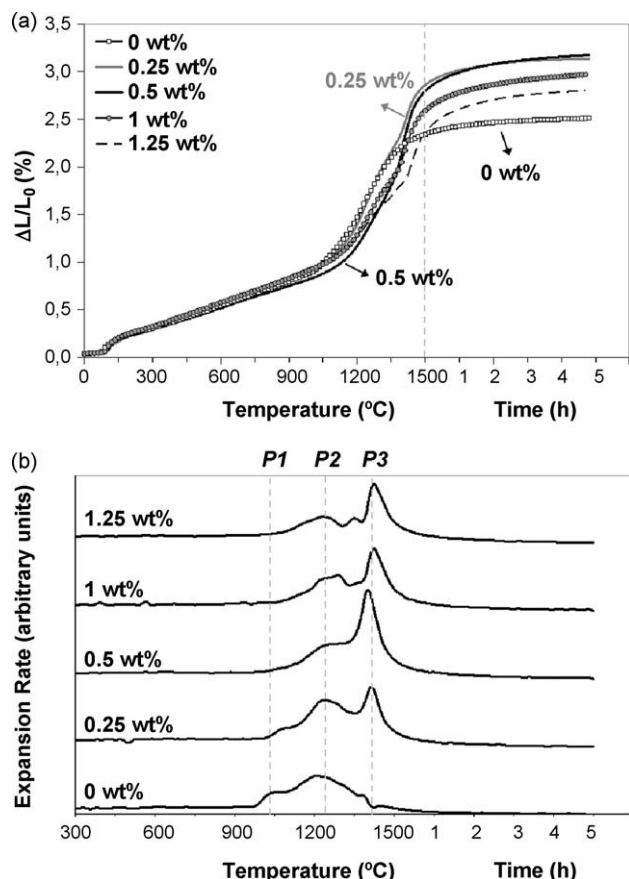


Fig. 1. (a) Expansion behavior and (b) expansion rate of alumina–magnesia castables containing different microsilica contents (0, 0.25, 0.5, 1 or 1.25 wt.%) and MgO < 45  $\mu\text{m}$ . The expansion rate peaks P1, P2 and P3 are related to the  $\text{CA}_2$ ,  $\text{MgAl}_2\text{O}_4$  and  $\text{CA}_6$  formation, respectively [7].

linear expansion levels (Fig. 1a), whereas further microsilica addition (1 and 1.25 wt.%) decreased the overall expansion. Additionally, a noteworthy reduction on the spinel expansion rate peak [12] was detected when increasing the microsilica content above 0.25 wt.% (Fig. 1b), showing its softening mechanism effect and better accommodation in the microstructure, during the spinel formation.

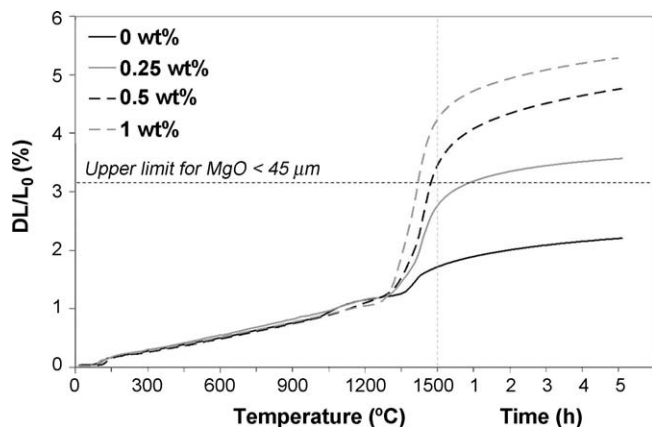


Fig. 2. Expansion behavior of alumina–magnesia castables containing a coarse magnesium source (<100  $\mu\text{m}$ ) and different microsilica contents (0, 0.25, 0.5 or 1 wt.%).

Considering these aspects, the objective of this work was to evaluate the effect of the microsilica content, for different MgO grain sizes (<45 and <100  $\mu\text{m}$ ), by means of expansion behavior, the microstructural features and their relationship with the physical and thermo-mechanical properties (apparent porosity, mechanical strength and creep resistance).

## 2. Materials and techniques

Alumina–magnesia castables containing different microsilica contents (0, 0.25, 0.5 or 1 wt.%) were designed using the Alfred particle packing model ( $q = 0.26$ ) [13]. The castables' matrix comprised 6 wt.% of dead-burnt magnesite (<45  $\mu\text{m}$  or <100  $\mu\text{m}$ , 95 wt.% MgO,  $\text{CaO/SiO}_2 = 0.37$ , Magnesita Refratários S.A., Brazil), 7 wt.% of reactive alumina (CL370, Almatiss, USA), 6 wt.% of calcium aluminate cement (Secar 71, Kerneos, France) and 18 wt.% of fine tabular alumina (<200  $\mu\text{m}$ , Almatiss, USA). To complement the compositions, coarse tabular alumina was used as aggregates ( $d \leq 6$  mm, Almatiss, USA).

To assess the spinel and the  $\text{CA}_6$  formation, an assisted sintering technique was carried out in a refractoriness-under-load equipment (Model RUL 421E, Netzsch, Germany). Cylindrical samples (50 mm  $\times$  50 mm) were prepared according to the 51053 DIN standard, cured at 50  $^\circ\text{C}$  and dried at 110  $^\circ\text{C}$  for 1 day, followed by pre-firing at 600  $^\circ\text{C}$  for 5 h before testing. For this evaluation, samples were heated up to 1500  $^\circ\text{C}$  under a heating rate of 3  $^\circ\text{C}/\text{min}$  and kept at this temperature for 5 h. The compression load applied was 0.02 MPa.

In the same equipment, creep tests were also performed in samples previously calcined at 600  $^\circ\text{C}$  and fired at 1550  $^\circ\text{C}$  for 24 h. The creep measurements were carried out at 1450  $^\circ\text{C}$  for 24 h under a constant compression load of 0.2 MPa. For the assisted sintering technique and creep resistance tests, two measurements were carried out for each sample.

For the microstructural evaluation, SEM analyses were conducted (SEM, Hitachi S-510, Tokyo, Japan). Furthermore, quantitative XRD analyses were carried out according to the Rietveld Method (TOPAS software). Regarding the physical properties, samples were cast (25 mm  $\times$  25 mm  $\times$  150 mm) to evaluate the modulus of rupture using MTS testing equipment

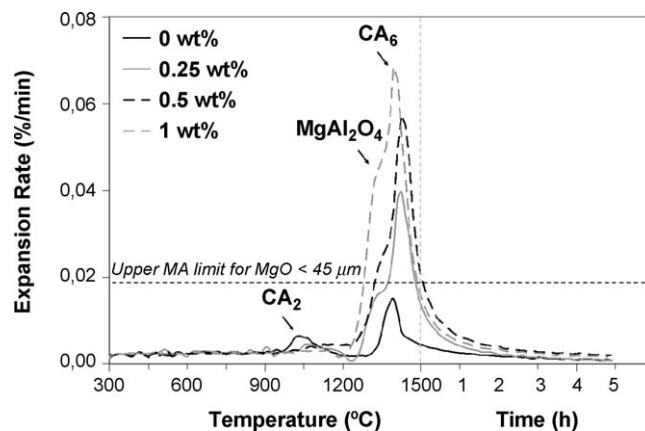


Fig. 3. Expansion rate of alumina–magnesia castables containing a coarse magnesium source (<100  $\mu\text{m}$ ) and different microsilica contents (0, 0.25, 0.5 or 1 wt.%). MA:  $\text{MgAl}_2\text{O}_4$ .

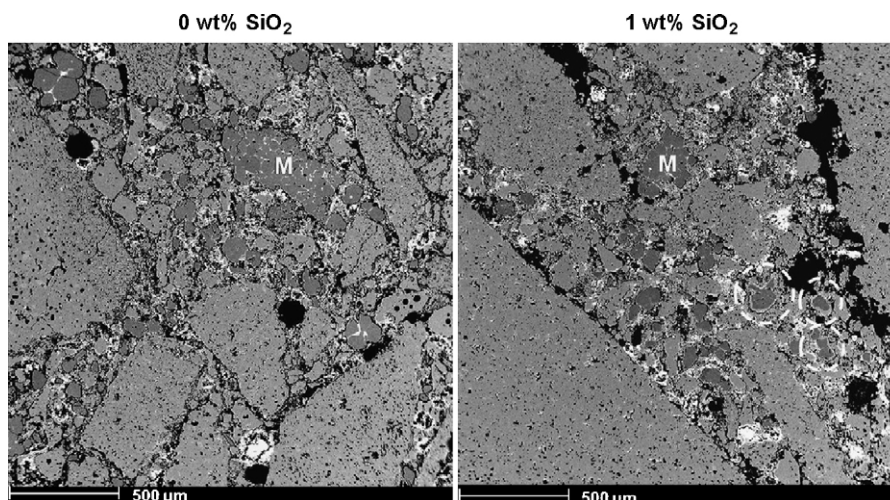


Fig. 4. Larger MgO grains left in the microstructure (M: dark gray grains) for the microsilica free alumina–magnesia castable with the coarsest MgO source ( $<100\text{ }\mu\text{m}$ ), after firing at  $1300\text{ }^{\circ}\text{C}$  for 5 h. The dotted circles indicate the reacted MgO grains for the 1 wt.% microsilica containing composition.

(MTS Systems, Model 810, USA) after firing at 1150, 1300 and  $1500\text{ }^{\circ}\text{C}$  for 5 h (heating rate =  $1\text{ }^{\circ}\text{C}/\text{min}$ ). Their permanent linear expansion (PLE) was measured by the percentage difference between the initial and the final length (before and after heat treatment) divided by the initial sample dimension. The 3-point bending test was carried out according to the ASTM C133-94

standard. The apparent porosity for the mechanical strength samples was also evaluated by the Archimedes technique in kerosene (after heat treatment at intermediate and high temperatures). For these physical properties measurements, five samples were evaluated for each firing temperature and the errors were calculated according to the standard deviation.

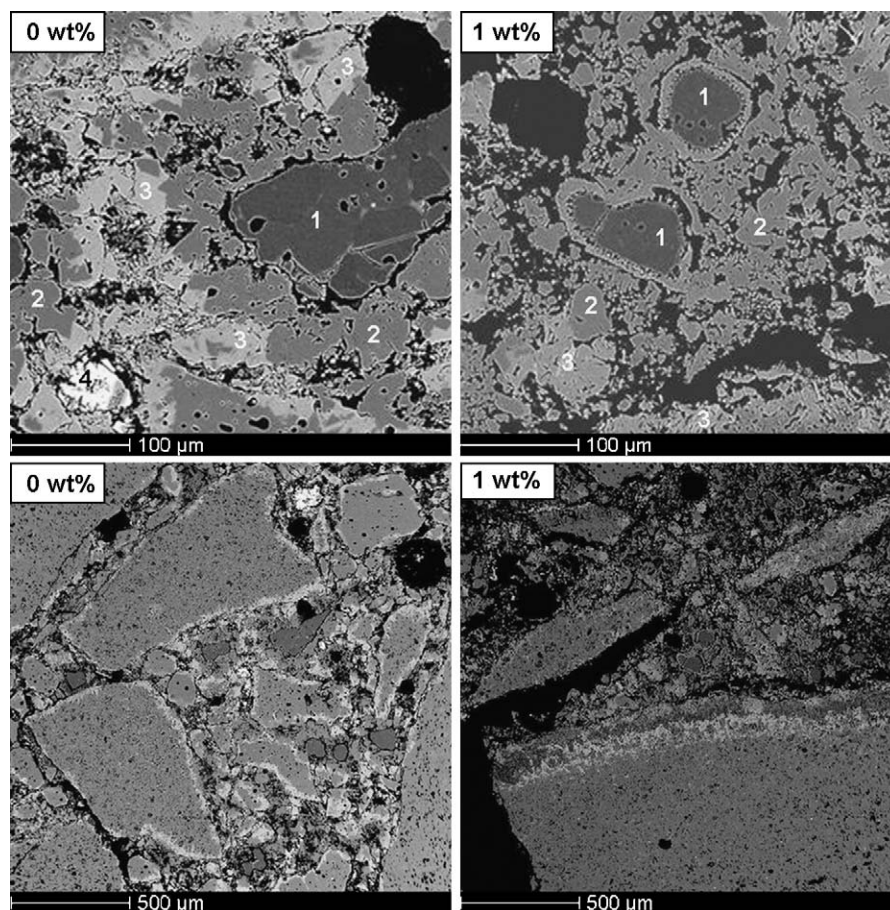


Fig. 5. Alumina–magnesia castables containing the coarsest MgO ( $<100\text{ }\mu\text{m}$ ) and different microsilica amounts (0 or 1 wt.%), after firing at  $1500\text{ }^{\circ}\text{C}$  for 5 h, where 1 = MgO, 2 =  $\text{MgAl}_2\text{O}_4$ , 3 =  $\text{CA}_6$  and 4 =  $\text{CA}_2$ .



### 3. Results and discussion

#### 3.1. Microsilica effect on $Al_2O_3$ –MgO castables containing coarse MgO grains

The overall expansion of the coarse MgO (<100  $\mu m$ ) alumina–magnesia castables scaled with the microsilica content increase (Fig. 2) leading to the following expansion ranking: 1 wt.% > 0.5 wt.% > 0.25 wt.% > 0 wt.%. According to the upper linear expansion limit for the fine MgO grain size (<45  $\mu m$ ) [7], shown as a dotted line in Fig. 2, only the microsilica free composition presented the same expansion range.

In order to evaluate the microsilica role in this sort of castables and understand which of the expansive phases –  $CA_2$ ,  $MgAl_2O_4$  or  $CA_6$  [7,12,14,15] – reaction rate was the most affected by this component, the derivative of the expansion curves is shown in Fig. 3. Among these three peaks, the  $MgAl_2O_4$  one was clearly influenced by the presence of microsilica. Compared to the upper spinel (MA) expansion peak rate limit for the fine MgO source (<45  $\mu m$ ), the mixture between high microsilica contents and the coarse MgO grain size seems to have spoiled the castables integrity leading to a huge expansion, large pores and a crack generation [10].

As higher microsilica contents resulted in higher spinel expansion peak rates, it could be stated that the liquid phase increased the  $Mg^{2+}$  dissolution and, therefore, sped up the spinel

formation. Moreover, this higher diffusion is also supported by the difference in the  $MgAl_2O_4$  peak starting temperature, which was close to 1200 °C for the 1 wt.% microsilica composition and near 1300 °C for the free microsilica one.

The microsilica ability in promoting the magnesia dissolution is pointed out by the SEM images presented in Fig. 4, for castables fired at 1300 °C for 5 h, where a higher amount of MgO grains left unreacted was detected for the microsilica free castable than for the 1 wt.% one. Additionally, a reaction layer at the edge of some magnesia grains was found for the microsilica containing castable, indicating its effect on the spinel formation kinetic rate. A third special feature is the spinel generation at the border of the magnesia grains instead at the edge of the alumina ones. By the Wagner mechanism [16], a faster  $Mg^{2+}$  diffusion to  $Al_2O_3$  should be expected. Nevertheless, due to a kinetic reason, the higher specific surface area of the reactive alumina prevailed and, therefore, led to this spinel formation mechanism in specific local areas.

After firing at a higher temperature (1500 °C for 5 h), the different kinetic behaviors for the microsilica containing castables (1 wt.%) or not (0 wt.%) are highlighted (Fig. 5) and provided further understanding of such a large difference on the overall expansion levels for these compositions (Fig. 2). For the microsilica free castable (0 wt.%), a homogeneous microstructure was developed and larger remnant MgO grains were detected. Thus, the lower dissolution in this case resulted in a

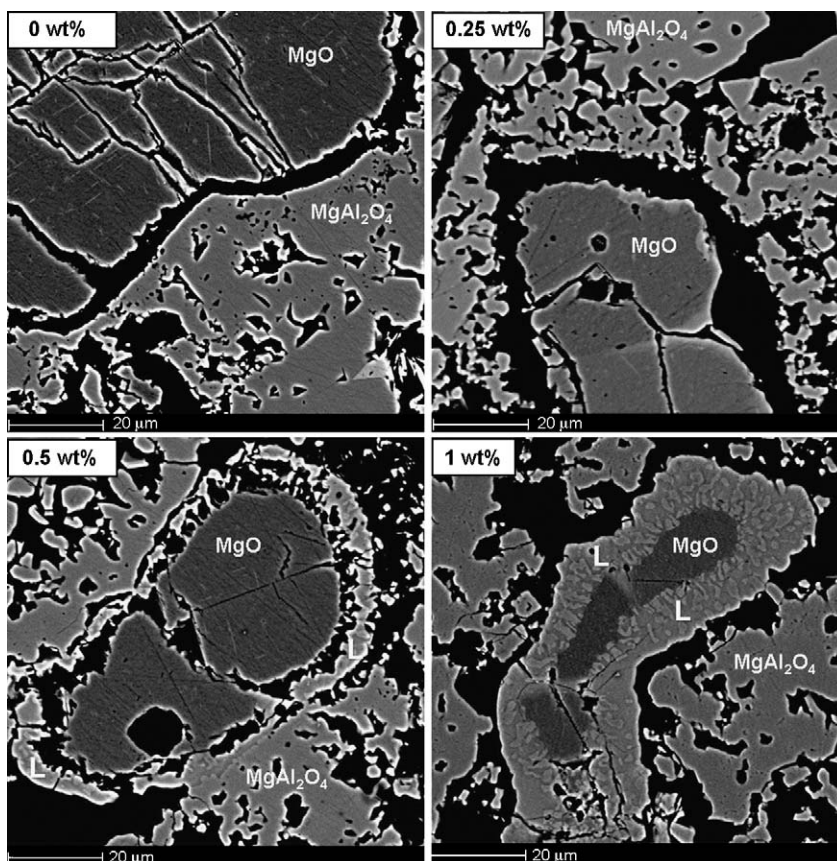


Fig. 6. Forsterite, monticellite and spinel reaction layer indicated by L in figure [10] at the edge of remnant MgO grains for the high microsilica containing castables (0.5 and 1 wt.%) and cracks at the MgO–spinel interface, after firing at 1500 °C for 5 h.

lower spinel content after the heating treatment (after 5 h firing at 1500 °C, only 13 wt.% of spinel was detected by XRD quantitative analyses) and, therefore, an easier accommodation of the expansive phases. Conversely, the microsilica speeding up kinetic effect led to 16 wt.% of spinel for the 1 wt.% SiO<sub>2</sub> castable. Furthermore, its highest spinel expansion peak rate intensity (Fig. 3) indicates a fast magnesia dissolution, leading to the generation of a higher amount of large pores and cracks (Fig. 5—1 wt.%). According to Kiyota [17] and Nakagawa et al. [18], the generation of pores, during the MgO diffusion and spinel formation, plays the main role on the overall expansion of alumina–magnesia castables.

A further aspect related to the interaction between microsilica and the coarse MgO source is that forsterite (Mg<sub>2</sub>SiO<sub>4</sub>) and monticellite (CaMgSiO<sub>4</sub>) are prone to be formed at high temperatures [10]. According to Fig. 6, a reaction layer at the edge of the magnesia grains is observed only for the castables containing 0.5 or 1 wt.% of microsilica. These phases were not detected for the 0 or 0.25 wt.% microsilica castables and only spinel was observed surrounding the MgO grains. For all compositions, cracks at the interface between the MgO grains and the spinel matrix were found, due to the thermal expansion coefficient mismatch between MgAl<sub>2</sub>O<sub>4</sub> and MgO, as previously discussed by Rigaud et al. [19].

Regarding the CA<sub>6</sub> formation, reducing the microsilica content led to the generation of equiaxed crystals, as observed for the fine MgO source [7] and also pointed out by An et al. [20]. This result is confirmed in Fig. 7, where the 0 and 0.25 wt.% microsilica castables presented equiaxed CA<sub>6</sub> grains instead of the usual CA<sub>6</sub> needle-like shape ones developed for the 0.5 and 1 wt.% microsilica compositions. Moreover, due to the slower spinel reaction kinetic by reducing the microsilica content, a greater amount of reactive alumina was available for the CA<sub>6</sub> formation, leading to higher CA<sub>6</sub> content values (21 wt.% of CA<sub>6</sub> for the 0 wt.% SiO<sub>2</sub>, 18 wt.% of CA<sub>6</sub> for the 0.25 or 0.5 wt.% SiO<sub>2</sub> and 16 wt.% of CA<sub>6</sub> for the 1 wt.% SiO<sub>2</sub> castable, according to XRD quantitative analyses for the samples fired at 1500 °C for 5 h). This feature is in tune with the results presented by Ide et al. [21], indicating higher CA<sub>6</sub> formation for coarse MgO grain sizes due to their lower dissolution and the resulting delay on the spinel formation.

### 3.2. Microsilica effect on Al<sub>2</sub>O<sub>3</sub>–MgO castables containing different MgO grain sizes

Microsilica played different roles on the expansive phase generation at high temperatures when the MgO grain size was changed (<45 and <100 μm). Fig. 8 shows the microsilica effect on the permanent linear expansion (PLE), apparent

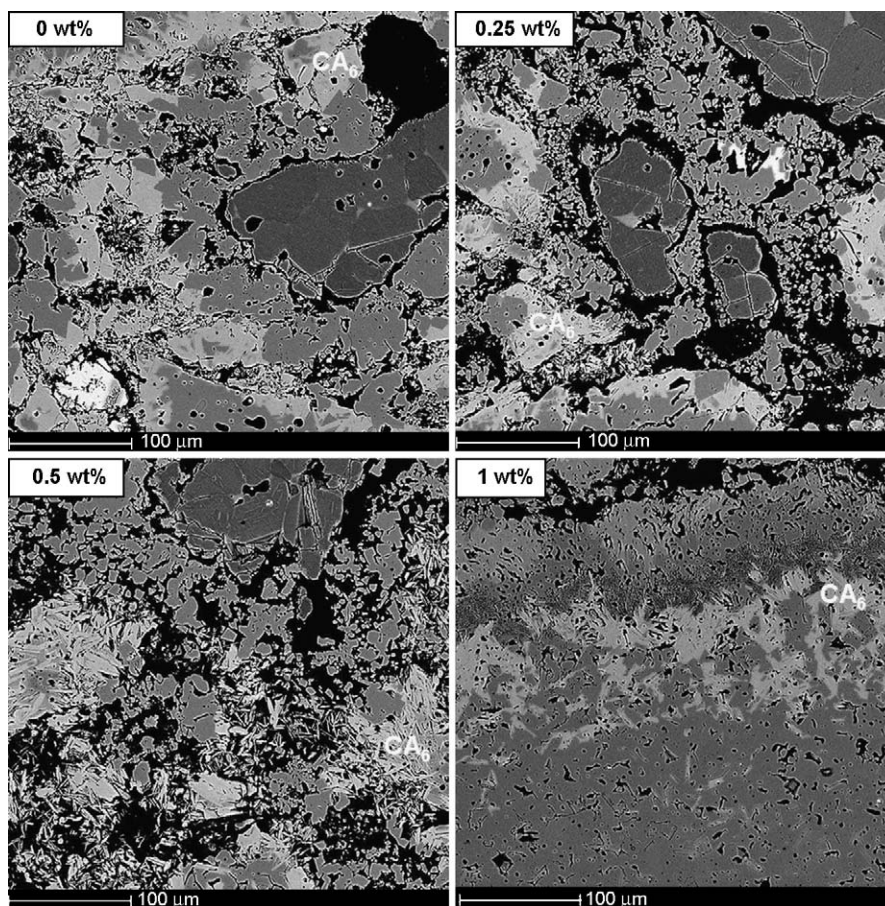


Fig. 7. CA<sub>6</sub> morphology for different microsilica contents: equiaxed (for 0 and 0.25 wt.% SiO<sub>2</sub>) and needle-like shape ones (for 0.5 and 1 wt.% SiO<sub>2</sub>) for castables fired at 1500 °C for 5 h.



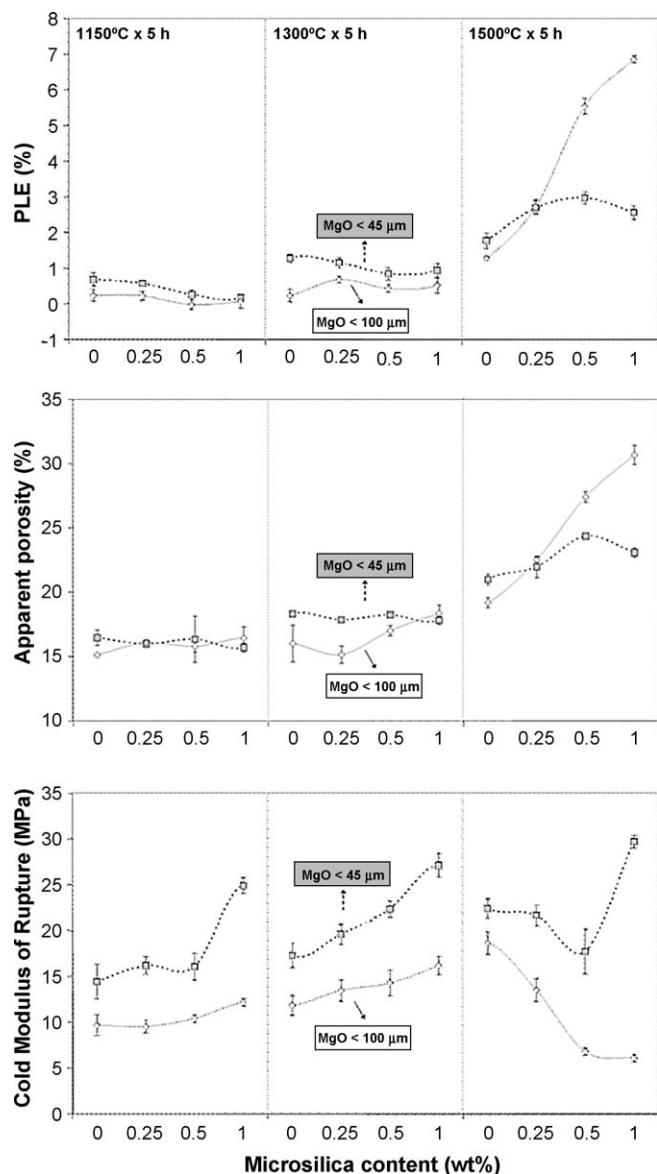


Fig. 8. Permanent linear expansion (PLE), apparent porosity (AP) and mechanical strength for the alumina–magnesia castables, containing different MgO grain sizes (<45 and <100 μm) and microsilica contents (0, 0.25, 0.5 and 1 wt.%), after firing at 1150, 1300 and 1500 °C for 5 h, respectively.

porosity (AP) and cold mechanical strength of these castables, after firing for 5 h at 1150, 1300 and 1500 °C, respectively. For the lowest temperature (1150 °C), a slightly higher PLE was detected for the microsilica free (0 wt.%) and for the 0.25 wt.% microsilica containing castables. This result is related to the  $CA_2$  formation due to a lack of competition between silica and alumina to react with calcia [7]. Nevertheless, all castables presented a lower linear expansion change range (0–1%) and the PLE values were close, regardless of the MgO grain size as lower spinel formation was expected for this temperature.

After firing at 1300 °C, microsilica imparted a particular effect for the different castables once more. Due to a faster reaction rate, all the PLE values were higher for the <45 μm MgO than for the <100 μm one. At this temperature, for the finer MgO source (<45 μm), higher silica contents resulted in

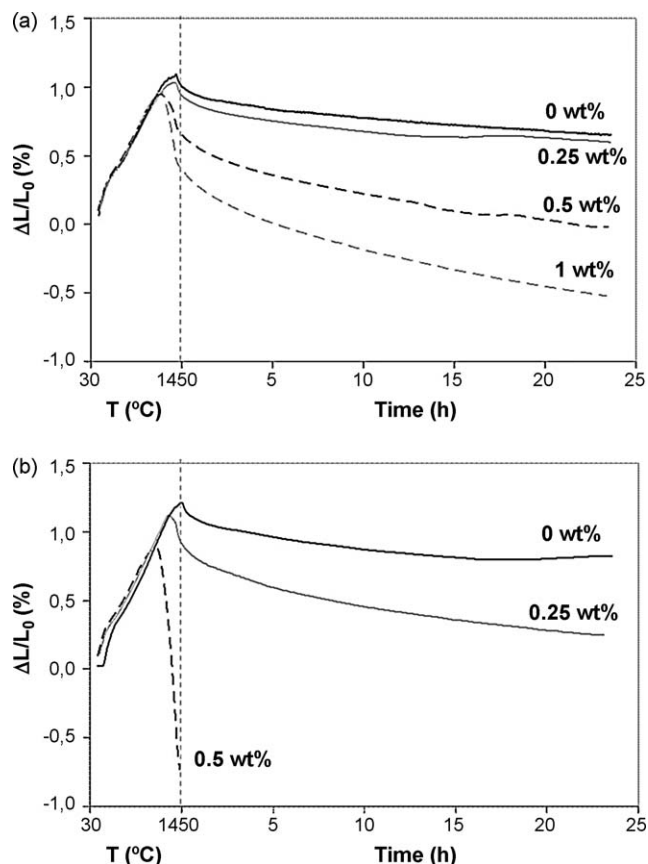


Fig. 9. Creep resistance for the alumina–magnesia castables, containing different microsilica contents (0, 0.25, 0.5 and 1 wt.%), for (a) MgO < 45 μm [7] and (b) MgO < 100 μm (1450 °C × 24 h, 0.2 MPa).

lower PLE, indicating its counterbalancing effect, as discussed by Myhre et al. [1] and by Yuanbing et al. [22]. Nevertheless, increasing the microsilica content for the coarse MgO containing castables led to a higher average PLE than the microsilica free one (0 wt.%), as a consequence of the faster  $Mg^{2+}$  dissolution in the presence of liquid.

These different microsilica effects are highlighted for the PLE results of the castables fired at 1500 °C. For the fine MgO grain size source, due to its faster dissolution, almost all of the expected generated spinel was developed after firing at 1300 °C [10]. Therefore, the observed PLE for this MgO grain size (<45 μm) at 1500 °C is mainly correlated to the  $CA_6$  formation. According to previous work [7], increasing the microsilica content up to 0.5 wt.% led to higher expansion, due to the higher  $CA_6$  generation and its needle-like shape crystals growth. However, due to the higher liquid formation, the 1 wt.% microsilica containing castable presented lower PLE when the MgO grain size was <45 μm.

Conversely, for the coarse MgO source (<100 μm) the spinel expansion is delayed and mostly developed at temperatures higher than 1300 °C as this source of magnesia presents lower specific surface area [10,21]. For this sort of castables, the expansion scaled with the microsilica content, indicating that microsilica not always accommodates the spinel expansion. Comparing the coarser MgO grain size with the finer one, the PLE values are close for the 0 and 0.25 wt.%

microsilica containing castables, but much higher for the 0.5 and 1 wt.% ones, pointing out the microsilica effects on speeding up the spinel formation and expansion. Furthermore, high microsilica contents also increase the  $CA_6$  expansion rate [7] and, therefore, resulted in the huge expansion detected for both compositions ( $MgO < 100 \mu m$ , containing 0.5 or 1 wt.% of microsilica).

As a consequence of these different behaviors according to the  $MgO$  grain sizes and microsilica content, the physical properties (apparent porosity and mechanical strength) of the castables were affected. Regarding the apparent porosity (AP), due to the lower expansion, there was practically no difference between the  $MgO$  grain sizes when the microsilica content is changed after firing at  $1150^\circ C$ . On the other hand, the higher spinel formation driving force for the fine  $MgO$  grain size ( $<45 \mu m$ ) led to higher AP levels than the coarse  $MgO$  grain size, after firing at  $1300^\circ C$ . Nevertheless, as the spinel formation and the decomposition of  $CA_2$  are carried out simultaneously for the coarse  $MgO$  grain size and both depend on the microsilica content, the AP effect at this temperature is not as clear as for the fine  $MgO$  grain size. Nevertheless, the microsilica effect for the coarse  $MgO$  grains is highlighted after firing at  $1500^\circ C$ , as lower silica content (0 and 0.25 wt.%) resulted in AP values in the same range than those observed for the fine  $MgO$  grain size, whereas the apparent porosity was much higher when increasing the microsilica amount (0.5 and 1 wt.%).

Concerning the mechanical strength, the finer  $MgO$  ( $<45 \mu m$ ) containing castables presented better performance than the coarser  $MgO$  ( $<100 \mu m$ ) ones, for all evaluated temperatures. For both  $MgO$  grain sizes, the cold modulus of rupture (CMOR) increased with the microsilica content at  $1150$  and  $1300^\circ C$ , most likely due to better packing and the higher amount of liquid phases (this aspect is going to be highlighted further by the creep resistance). After firing at  $1500^\circ C$ , the expansion and the cracking generation reduced the CMOR when the microsilica amount increased for both  $MgO$  grain sizes, except for the fine  $MgO < 45 \mu m$  containing 1 wt.% of microsilica. The mechanical strength was specially spoiled for the coarse  $MgO$  castables due to their huge expansion. For the fine  $MgO$  compositions, a reduction in the mechanical strength was detected up to 0.5 wt.%  $SiO_2$ , due to the higher  $CA_6$  expansion rate (Fig. 1), whereas in the castable containing 1 wt.% of microsilica, the sintering effects led to a lower expansion, lower porosity and consequently a higher cold modulus of rupture.

As the microsilica addition and the liquid phase generated lead to refractoriness drawbacks, the creep resistance was also evaluated (Fig. 9). Regardless of the  $MgO$  grain sizes, the creep scaled with the increase in the microsilica content. However, for the coarser  $MgO$  grain size a worsening of the creep behavior for the compositions containing 0.25 or 0.5 wt.% microsilica was detected when compared to the fine  $MgO$  source ( $<45 \mu m$ ). As a consequence of the huge creep values for the 0.5 wt.%  $SiO_2$  castable ( $MgO < 100 \mu m$ ), it was not possible to analyze the alumina–magnesia castable containing 1 wt.% of microsilica, due to its high expansion, porosity and cracking extent.

#### 4. Conclusions

Due to the different microsilica roles pointed out, this work highlighted that a sound conclusion regarding its behavior in  $Al_2O_3$ – $MgO$  refractory castables is not straightforward. When using fine magnesia grain sizes ( $<45 \mu m$ ), microsilica behaved as expected and reported by the literature, counterbalancing the *in situ* spinel expansion. On the other hand, for the coarse  $MgO$  grain size ( $<100 \mu m$ ), silica sped up the spinel formation, leading to a huge expansion and worsened the physical properties after thermal treatment at  $1500^\circ C$  for 5 h. Therefore, the need for a systemic approach for alumina–magnesia castables is clear, as different parameters could affect their expansion design.

#### Acknowledgements

The authors are grateful to the Federation for International Refractory Research and Education (FIRE) and its industrial partners: Alcan (France), Alcoa (US), Almatix (Germany), ANH (US), Calderys (France), Magnesita S.A. (Brazil), Kerneos (France), Tata Steel–Corus (Netherlands), and the Brazilian Research Funding FAPESP for supporting this work. Furthermore, the authors are thankful to Prof. M. Rigaud for his comments and to D.H. Milanez and E.Y. Sako for the castable processing.

#### References

- [1] B. Myhre, B. Sandberg, A.M. Hundere, Castables with  $MgO$ – $SiO_2$ – $Al_2O_3$  as bond phase, in: Proceedings of XXVI ALAFAR Congress, Asociacion Latinoamericana de Fabricantes de Refractarios, San Juan, Puerto Rico, (1997), p. 10.
- [2] P. Nandi, A. Grag, B.D. Chatteraj, M.S. Mukhopadhyay, Effect of silica and temperature on spinel-based high-alumina castables, American Ceramic Society Bulletin 31 (12) (2000) 65–69.
- [3] B. Nagai, O. Matsumoto, T. Isobe, Development of high-alumina castable for steel ladles (findings on spinel formation in alumina–magnesia castable), Taikabutsu Overseas 10 (1) (1990) 23–28.
- [4] M. Kobayashi, K. Kataoka, Y. Sakamoto, I. Kifune, Use of alumina–magnesia castables in steel ladles sidewalls, Taikabutsu Overseas 17 (3) (1997) 39–44.
- [5] M. Nanba, T. Kaneshige, Y. Hamazaki, H. Nishio, I. Ebizawa, Thermal characteristics of castables for teeming ladles, Taikabutsu Overseas 16 (3) (1996) 17–21.
- [6] Y.C. Ko, Properties and production of  $Al_2O_3$ –spinel and  $Al_2O_3$ – $MgO$  castables for steel ladles, Ceramic News 6 (1) (2002) 51–56.
- [7] M.A.L. Braulio, L.R.M. Bittencourt, J. Poirier, V.C. Pandolfelli, Microsilica effects on cement bonded alumina–magnesia refractory castables, Journal of the Technical Association of Refractories-Japan 28 (3) (2008) 180–184.
- [8] M. Tawara, K. Fuji, T. Taniguchi, M. Hagiwara, T. Kibayashi, M. Tanaka, Application of alumina–magnesia castable in high temperature steel ladles, Taikabutsu Overseas 16 (2) (1996) 17–19.
- [9] M.A.L. Braulio, J.F.R. Castro, C. Pagliosa, L.R.M. Bittencourt, V.C. Pandolfelli, From macro to nanomagnesia: designing the *in situ* spinel expansion, Journal of the American Ceramic Society 91 (9) (2008) 3090–3093.
- [10] M.A.L. Braulio, L.R.M. Bittencourt, V.C. Pandolfelli, Magnesia grain size effect on *in situ* spinel refractory castables, Journal of the European Ceramic Society 28 (2008) 2845–2852.
- [11] F. Simonin, C. Olagnon, S. Maximilien, G. Fantozzi, L.A. Diaz, R. Torrecillas, Thermomechanical behavior of high-alumina refractory

- castables with synthetic spinel additions, *Journal of the American Ceramic Society* 83 (10) (2000) 2481–2490.
- [12] M.A.L. Brulio, D.H. Milanez, E.Y. Sako, L.R.M. Bittencourt, V.C. Pandolfelli, Expansion behavior of cement bonded alumina–magnesia refractory castables, *American Ceramic Society Bulletin* 86 (12) (2007) 9201–9206.
- [13] R.G. Pileggi, A.R. Studart, M.D.M. Innocentini, V.C. Pandolfelli, High-performance refractory castables, *American Ceramic Society Bulletin* 81 (6) (2002) 37–42.
- [14] J.M. Auvray, C. Gault, M. Huger, Evolution of elastic properties and microstructural changes versus temperature in bonding phases of alumina and alumina–magnesia refractory castables, *Journal of the European Ceramic Society* 27 (2007) 3489–3496.
- [15] Y.C. Ko, J.T. Lay, Thermal expansion characteristics of alumina–magnesia and alumina–spinel castables in the temperature range 800°–1650 °C, *Journal of the American Ceramic Society* 83 (11) (2000) 2872–2874.
- [16] R.E. Carter, Mechanism of solid-state reaction between magnesium oxide and aluminum oxide and between magnesium oxide and ferric oxide, *Journal of the American Ceramic Society* 44 (3) (1997) 116–120.
- [17] Y. Kiyota, Reduction of permanent linear change of  $\text{Al}_2\text{O}_3$ –MgO castable, in: *Proceedings of UNITECR'07*, The German Refractories Association (GRA), Dresden, Germany, (2007), pp. 546–549.
- [18] Z. Nakagawa, N. Enomoto, T. Yi, K. Asano, Effect of corundum/periclase sizes on expansion behavior during synthesis of spinel, in: *Proceedings of UNITECR'95*, The Technical Association of Refractories-Japan, Kyoto, Japan, (1995), pp. 379–386.
- [19] M. Rigaud, S. Palco, N. Wang, Spinel formation in the  $\text{MgO}$ – $\text{Al}_2\text{O}_3$  relevant to basic oxides, in: *Proceedings of UNITECR'95*, The Technical Association of Refractories-Japan, Kyoto, Japan, (1995), pp. 387–394.
- [20] L. An, H.M. Chan, K.K. Soni, Control of calcium hexaluminate grain morphology in *in-situ* toughened ceramic composites, *Journal of Materials Science* 31 (1996) 3223–3229.
- [21] K. Ide, T. Suzuki, K. Asano, T. Nishi, T. Isobe, H. Ichikawa, Expansion behavior of alumina–magnesia castables, *Journal of the Technical Association of Refractories-Japan* 25 (3) (2005) 202–208.
- [22] L. Yuanbing, T. Xueguang, L. Yawei, H. Xueqin, L. Zhongxing, Z. Lei, Y. Bihui,  $\text{Al}_2\text{O}_3$ –MgO precast block used in steel ladle for LC and ULC steel, *Ceramic Forum International* 85 (10) (2008) E83–E85.